

**SPATIAL CORRELATIONS BETWEEN SILICATE AND METAL WEATHERING IN ANTARCTIC CHONDRITES.** E. D. Steer<sup>1</sup>, S. P. Schwenzer<sup>1</sup>, I. P. Wright<sup>1</sup>, M. M. Grady<sup>1</sup>, <sup>1</sup>Department of Physical Sciences, The Open University, Walton Hall, Milton Keynes, United Kingdom, MK7 6AA. ([beth.steer@open.ac.uk](mailto:beth.steer@open.ac.uk))

**Introduction:** Terrestrial alteration of Antarctic meteorites is a long documented phenomenon [e.g. 1,2] and has been frequently used as an analogue for weathering on Mars [3,4]. Focused reports of separate alteration effects have been thorough [5], but this work is part of a larger study aiming to consolidate mineralogical alteration, trace and major element inventories, noble gas inventories and halogen contents in order to correlate the visible with the non-visible effects. Ultimately, we hope to use what we have learnt from Antarctic weathering to interpret alteration of Martian surface rocks.

Here we report data to link the etching and compositional alteration of olivines with the weathering of kamacite and taenite and the consequent staining of the meteorite. Over 250 olivines in a rim and an interior sample of a meteorite have been measured and compared with elemental maps and back scattered electron images to build up a picture of the exact locations and possible causes of compositional variation.

**Samples:** The samples in this study are rim and interior thin sections of the L6 ordinary chondrite Queen Alexandra Range 94214, given the designations QUE 94214, 10 (rim) and QUE 94214, 8 (interior). The chondrite has a weathering grade of B/C [6].

**Methods:** Reflectance and transmitted light microscopy was performed to get an overview of the sample texturally and mineralogically. A FEI Quanta 3D dual beam scanning electron microscope fitted with an Oxford Instruments 80 mm X-MAX energy dispersive X-ray detector was used at The Open University to obtain images and element maps. From these, maps were drawn (Fig. 1). Mineral analysis was obtained from a Cameca SX100 at The Open University under the following conditions: spot size 10  $\mu\text{m}$ , accelerated voltage 20 kV, beam current 20 nA.

**Petrology:** We confirmed classification of this chondrite as an L6 chondrite based on compositions of pyroxenes, olivines and chromites and textural analysis. Mineral phases in both rim and interior are: olivine (37.3 vol. %,  $\text{Fa}_{22-26}$ ), low Ca pyroxenes (24.7 vol. %,  $\text{En}_{78}\text{Fs}_{22}\text{Wo}_2$ ), microcrystalline intergrowth of feldspar, olivine and pyroxene (14.1 vol. %), feldspar (10.9 vol. %,  $\text{An}_9\text{Ab}_{84}\text{Or}_7$ ), fized troilite (5.0 vol. %), polycrystalline kamacite (3.1 vol. %), taenite (1.27 vol. %), accessory phases (6.73 vol. %) chromite, chlorapatite, whitlockite.

Chondrule fragments are indistinct in the meteorite and merge with the groundmass of olivine, pyroxene,

minor feldspar, troilite, Fe-Ni metal, phosphates and chromite. Fusion crust is present on one side of the rim sample. The rim sample (94214, 10) has ubiquitous iron staining, the interior sample (94214, 8) has iron staining covering over 40% of the sample following altering metal particles, which are ringed by blood red limonite products. These alteration products then follow veins along fractures in the olivine and pyroxene crystals.

SEM analysis shows that the phases visibly weathering in both rim and interior are kamacite, taenite and troilite with the more Fe-rich kamacite phases altering preferentially, often leaving behind the more Ni-rich metals. Resultant products are Fe-oxyhydroxides forming halos around the weathering minerals and in veins and voids. These contain little S from the troilite, which is assumed to have been largely removed from the meteorite [7]. Olivine crystals can be seen in SEM images ( $\mu\text{m}$  scale) to be forming etch pits, often in crystals adjacent to where metal grains are weathering. Areas adjacent to weathering troilite are often more affected. Fractures are pervasive through the meteorite, concentrating in olivines in the form of planar fractures. Olivine and pyroxene contacts often have intramineral fractures running along them. These fractures serve to allow the propagation of veins and are expanded chemically as can be seen by dendritic saw-tooth edges.

Over 130 olivines from the rim section and 120 from the interior sample were measured by EMPA. Spatially resolved compositional data from the exterior sample (QUE 94214 10) shows an increase in range of FeO weight % content of olivines with decreasing distance to the rim of the meteorite (Fig. 2). Within 500  $\mu\text{m}$  of the fusion crust, the olivine FeO weight % spread increased to 21.5–24.5. Between 500–2300  $\mu\text{m}$  the spread decreased to 21.5–23, 2300–3000  $\mu\text{m}$ , the range decreases to 21.5–22.5.

In the interior sample, olivine FeO weight % has a greater spread in areas of iron staining (Fig. 3). There is also an increase in FeO compositional range in the interior of the meteorite in proximity to metal degradation (Fig. 1, Fig. 3).

This is accompanied by an overall systematic decrease of 0.6 FeO weight % and increase of MgO weight % by 0.5 with 600  $\mu\text{m}$  distance from the fusion crust.

**Discussion and conclusions:** The presence of iron staining and alteration products creates a heterogene-

ous distribution of olivine alteration and leaching that does not solely depend on distance from the rim of the sample. While olivine crystals within the first 500  $\mu\text{m}$  from the fusion crust show the most changes in Fe-concentrations, the local composition beyond is controlled by local weathering products. However, on a wider scale, there is a small overall decrease of iron with the distance from the fusion crust and an increase of MgO weight %, reflecting the relative mobility of the cations in the weathering system [8]. The areas of iron staining occur in close proximity to the grains from which the iron originated, e.g. decomposing taenite, kamacite and troilite grains. The preferential alteration of silicates adjacent to altering troilite may be due to the liberation of S from the troilite, which is not included in the alteration products, creating more acidic fluids which speeds the alteration of surrounding silicates. The veins from the altering grains propagate along pre-existing planar fractures, formed by shock prior to weathering [9], dominantly penetrating through olivines and pyroxenes. The veins also travel along intramineral fractures likely formed by different thermal expansion coefficients of the mineral species, due to diurnal fluctuation of temperature [10]. Areas with little metal present, such as the silicate-dominated chondrule remnants, are less altered and yield olivine compositions with less variation. The presence of the weathering Fe-metal grains and troilite further facilitates the weathering of surrounding silicates by forming

porous pathways for more fluid to travel [11]. The forming of etch pits and sawtooth edges of olivine surrounding metal grains, troilite and their alteration products are visible evidence of the effect weathering metals are having on the silicates in the meteorite and the beginnings of the adsorption of olivine [11,12]. In conclusion, beyond the initial 500  $\mu\text{m}$  from the outer edge, the controlling factor is local weathering products, and an interior meteorite sample is not a guarantee of more pristine silicates.

**References:** [1] Gooding, J. (1982) *LPSC XII*, 1105-1122. [2] Velbel, M.A. (1988) *Meteoritics*, 23, 151-159. [3] Chevrier, V. et al. (2006) *EPSL*, 244, 501-514. [4] Hallis, L.J. (2013) *Meteoritics and Planetary Science*, 48, 165-179. [5] Velbel, M.A. (2012), *MAPS*. [6] The Meteoritical Bulletin, Accessed 22/11/13. [7] Lee, M. and Bland, P. (2004) *Geochimica et Cosmochimica Acta*, 68, 893-916. [8] Bland, P. et al. (2006) *Meteorites and the early solar system II*, pp 853-867. [9] Stöffler, D. et al. (1991) *Geochimica et Cosmochimica Acta*, 55, 3845-3867. [10] Andre, M. F. et al. (2004) *Polar Geography*, 28, 43-62. [11] Lee, M. et al. (2012) *MAPS*, 48,2, 224-240. [12] Velbel, M.A. and Barker, W.W. (2008) *Clays and Clay minerals*, 56, 112-127.

**Acknowledgements:** We thank the Antarctic Meteorite Working Group for allocation of samples and additional information.

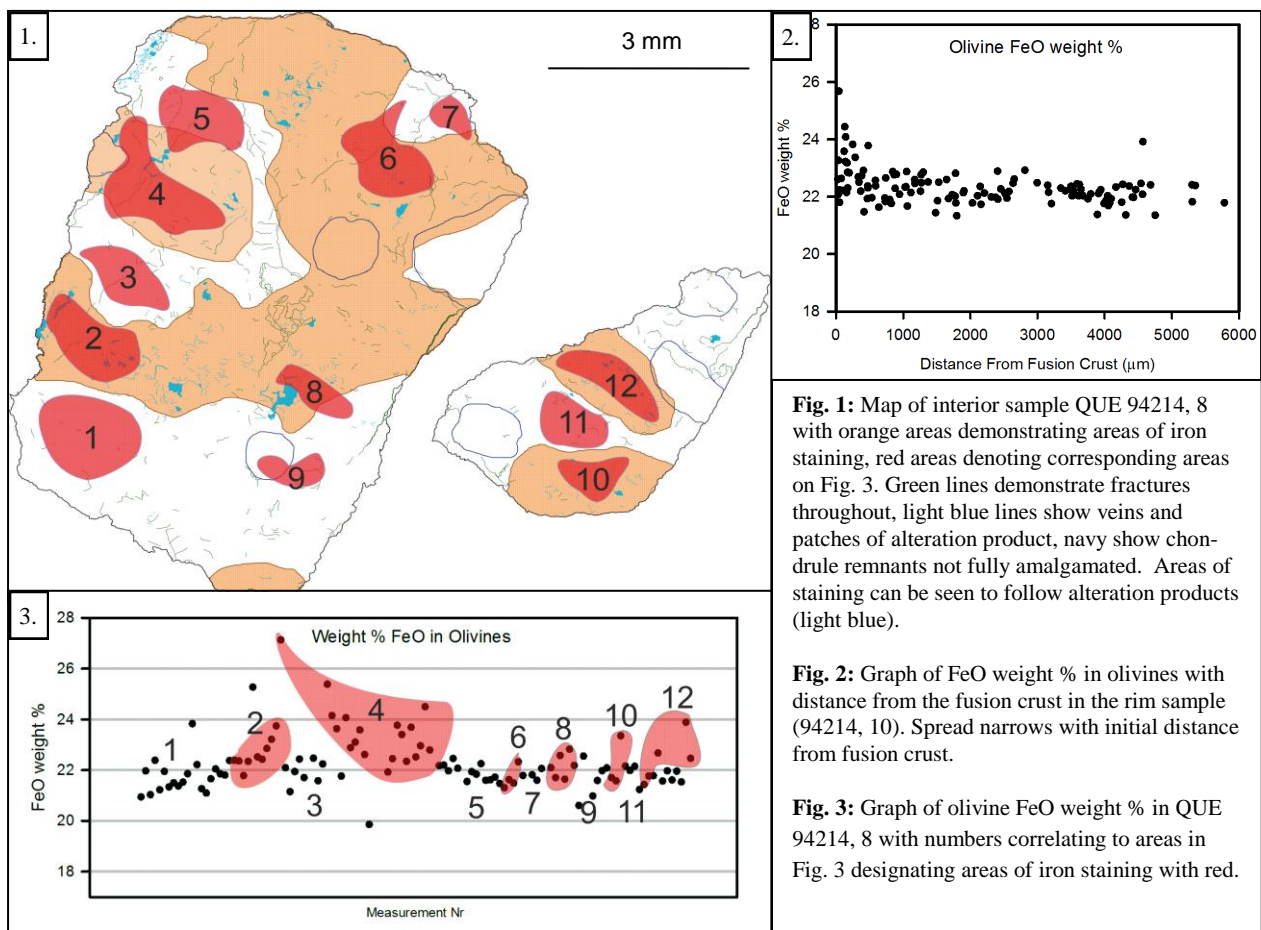


**Fig. 1:** Map of interior sample QUE 94214, 8 with orange areas demonstrating areas of iron staining, red areas denoting corresponding areas on Fig. 3. Green lines demonstrate fractures throughout, light blue lines show veins and patches of alteration product, navy show chondrule remnants not fully amalgamated. Areas of staining can be seen to follow alteration products (light blue).

**Fig. 2:** Graph of FeO weight % in olivines with distance from the fusion crust in the rim sample (94214, 10). Spread narrows with initial distance from fusion crust.

**Fig. 3:** Graph of olivine FeO weight % in QUE 94214, 8 with numbers correlating to areas in Fig. 3 designating areas of iron staining with red.